Research in Astron. Astrophys. **2011** Vol.**11** No.**3**, 293–308
http://www.raa-journal.org *http://www.iop.org/journals/raa*

Research in Astronomy and Astrophysics

Winding sense of galaxies around the local supercluster

Binil Aryal

Central Department of Physics, Tribhuvan University, Kirtipur, Nepal; *binil.aryal@uibk.ac.at*
Institut of Astro- and Particle Physics, Innsbruck University, Technikerstrasse 25, A-6020 Innsbruck, Austria

Received 2010 January 16; accepted 2010 October 22

Abstract We present an analysis of the winding sense (S and Z-shapes) of 1 621 field galaxies that have radial velocity between 3 000 km s^{-1} and 5 000 km s^{-1}. The preferred alignments of S- and Z-shaped galaxies are studied using chi-square, auto-correlation and Fourier series tests. We classify all the galaxies into 32 subsamples and notice a good agreement between the position angle (PA) distribution of the S- and Z-shaped galaxies. The homogeneous distribution of the S- and Z-shaped galaxies is more noticeable for the late-type spirals (Sc, Scd, Sd and Sm) than for the early-types (Sa, Sab, Sb and Sbc). A significant dominance of S-mode galaxies is apparent in the barred spirals. A random alignment is evident in the PA-distribution of Z- and S-mode spirals. In addition, a homogeneous distribution of the S- and Z-shaped galaxies is found to be invariant under global expansion. The PA-distribution of the total S-mode galaxies is found to be random, whereas a preferred alignment is clear for all the Z-mode galaxies. It is found that the galactic planes of Z-mode galaxies tend to lie in the equatorial plane.

Key words: galaxies: spiral — galaxies: clusters: individual (local supercluster)

1 INTRODUCTION

Differential rotation in a galaxy's disk generates density waves, leading to spiral arms. According to gravitational theory, the spiral arms start as leading modes but subsequently are transformed into trailing modes. With the passage of time, the spiral pattern gradually deteriorates by the differential rotation of the equatorial plane of the galaxy, but the bar structure persists for a long time (Oort 1970a). This structure can again regenerate the spiral pattern in the outer region. Thus, a close relation between the origin of the arms in the spirals and barred spirals cannot be denied (Oort 1970b).

Land et al. (2008) studied the distribution of projected spin vectors in $\sim$ 37 000 spiral galaxies taken from the Sloan Digital Sky Survey. They did not notice any evidence for an overall preferred handedness of the Universe. In a similar study, Longo (2007) found evidence for a preferred axis. Sugai & Iye (1995) used statistics and studied the winding sense of galaxies (S- and Z-patterns) in 9 825 spirals. No significant dominance from a random distribution was noticed. Aryal & Saurer (2005) studied the spatial orientations of spin vectors in 4 073 galaxies in the Local Supercluster. No preferred alignment was noticed for the total sample. These results hint that the distribution of the angular momentum of galaxies is entirely random in two-dimensional (S- and Z-shaped) and three-dimensional (spin vector) analysis, provided that the database is rich enough.

In order to understand the true structural modes (leading or trailing) of spiral galaxies, we need to know the direction of the spiral pattern (S- or Z-patterns), the approaching and receding sides and the near and far parts, since galaxies are commonly inclined in space with respect to the line of sight. The S- and Z-patterns can be determined from the image of the galaxy. Similarly, the approaching and receding sides can be defined if spectroscopy data on rotation are available. The third one is fairly hard to establish. For this, Pasha (1985) used 'tilt' criteria and studied the sense of winding of the arms in 132 spirals. He found 107 spirals have a trailing arm. Thomasson et al. (1989) theoretically studied this subject and performed N-body simulations in order to understand the formation of spiral structures in retrograde galaxy encounters. Interestingly, they noticed the importance of halo mass. They concluded that the spirals having halos with masses larger than the disk mass exhibit a leading pattern. Thus, the makeup of galactic haloes is important to cosmology in order to understand the evolution of galaxies.

By considering the group of transformations acting on the configuration space, Capozziello & Lattanzi (2006) predicted that the progressive loss of inhomogeneity in the S- and Z-shaped galaxies might have some connection with the rotationally-supported (spirals, barred spirals) and randomized stellar systems (lenticulars, ellipticals).

The preferred alignments of galaxies can be an indicator of initial conditions when galaxies and clusters formed, provided that the angular momenta of galaxies have not been altered too much since their formation. A useful property of galaxies in clusters for which theories make different predictions is the angular momentum distribution. The 'Pancake model' by Doroshkevich (1973), the 'Hierarchy model' by Peebles (1969) and the 'Primordial vorticity model' by Ozernoy (1978) predict different scenarios concerning the formation of large-scale structure. Thus, the study of galaxy orientation has the potential to yield important information regarding the formation and evolution of cosmic structures. In this work, we present an analysis of the winding sense and preferred alignments of galaxies that have radial velocity (RV) 3 000 km s^{-1} to 5 000 km s^{-1}. These are field galaxies. We intend to study the importance of the winding sense in order to understand the true structural modes (i.e., leading and trailing arm) of the galaxy. We expect to study the following: (1) Is the distribution of S- and Z-shaped galaxies homogeneous in the field? (2) Is there any correlation between the preferred alignment and the winding sense of galaxies? (3) Does radial velocity dependence exist concerning the winding sense of galaxies? And finally, (4) What can we say about the distribution of the true structural modes (i.e., the leading or trailing arm) of galaxies regarding the large scale structure?

This paper is organized as follows: In Section 2 we describe the method of data reduction. In Section 3 we give a brief account of the methods and the statistics used. Finally, a discussion of the statistical results and the conclusions are presented in Sections 4 and 5, respectively.

2 THE SAMPLE: DATA REDUCTION

Eighteen catalogs were used for the data compilation. A list of the catalogs and their references are given in Table 1. The abbreviations given in the first column of Table 1 are as follows: NGC - New General Catalog, UGC - Uppsala General Catalog of Galaxies, ESO - ESO/Uppsala Survey of the ESO (B) Atlas, IC - Index Catalog, MCG - Morphological Galaxy Catalog, UGCA - Uppsala obs. General Catalog, Addendum, CGCG - Catalog of Galaxies and Clusters of Galaxies, KUG - Kiso Ultraviolet Galaxy Catalog, MRK - Markarian Galaxy Catalog, MESSIER - Catalogue des nebuleuses et des amas d'etoiles, BCG - Brandner+Grebel+Chu Catalog, LSBG - Low Surface Brightness Galaxies, SBS - Second Byurakan Survey, LCRS - Las Companas Red Shift Survey, DDO - David Dunlap Observatory Publications, IRAS - Infrared Astronomical Satellite, SGC - Southern Galaxy Catalog and UM - University of Michigan: Curtis Schmidt-thin prism survey for extragalactic emission-line objects: List I-V.

Table 1 List of Catalogs Used for the Data Compilation

Catalogue	*N*	Reference
NGC	623	Dreyer (1895, 1908)
UGC	276	Nilson (1973)
ESO	123	Lauberts (1982)
IC	93	Dreyer (1895, 1908)
MCG	88	Vorontsov-Vel'Yaminov et al. (1962–1974)
UGCA	84	Nilson (1974)
CGCG	75	Zwicky et al. (1961–1968)
KUG	44	Takase (1980–2000)
MRK	40	Markarian (1967)
MESSIER	41	Messier (1784)
BCG	28	Brandner et al. (2000)
LSBG	23	Impey et al. (1996)
SBS	17	Markarian et al. (1983)
LCRS	16	Shectman et al. (1996)
DDO	15	Bergh (1959, 1966)
IRAS	15	Infrared Astronomical Satellite (1983)
SGC	10	Corwin et al. (1985)
UM	10	MacAlpine et al. (1977a,b,c, 1978, 1981)

The first column lists the abbreviation of catalogs. The second column gives the total number of galaxies. The references are listed in the last column.

The NASA/IPAC extragalactic database (NED, *http://nedwww.ipac.caltech.edu/*) was used to compile these catalogs. The main selection process was as follows: First, galaxies having RVs in the range 3 000 km s^{-1} to 5 000 km s^{-1} were collected. We downloaded the images of all these galaxies from NED in FITS format. The second step was to compile the morphology of these galaxies from the catalog. Any galaxy with doubtful morphology (e.g., 'S', 'S0' or 'Sa') was omitted. Finally, the position angles (PAs) of galaxies were added from the UGC, ESO, and Third Reference Catalog of Bright Galaxies (de Vaucouleurs et al. 1991).

There were two clusters, Abell 0426 (α(J2000) = $03^{\rm h}18^{\rm m}\ 36.4^{\rm s}$, δ(J2000) = $+41^\circ30'54''$) and Abell 3627 (α(J2000) = $16^{\rm h}15^{\rm m}32.8^{\rm s}$, δ(J2000) = $-60^\circ54'30''$), in our region. These clusters have mean RVs 5 366 km s^{-1} (75 $\pm$ 5 Mpc) and 4 881 km s^{-1} (63 $\pm$ 4 Mpc), respectively (Abell et al. 1989; Struble & Rodd 1999). We removed the galaxies belonging to the cluster Abell 0426 using the catalog established by Brunzendorf & Meusinger (1999). For the cluster Abell 3627 galaxies, we used the Photometric Atlas of Northern Bright Galaxies (Kodaira et al. 1990) and the Uppsala Galaxy Catalog (Nilson 1973). There were 174 galaxies belonging to these clusters in our database, which we removed.

The RVs were compiled from the Las Campanas Redshift Survey (Shectman 1996). The PAs and the diameters of galaxies were added from the Uppsala Galaxy Catalog (Nilson 1973), the Uppsala obs. General Catalog, its Addendum (Nilson 1974), the Photometric Atlas of Northern Bright Galaxies (Kodaira et al. 1990), the ESO/Uppsala Survey of the European Southern Observatory (Lauberts 1982), the Southern Galaxy Catalog (Corwin et al. 1985) and the Third Reference Catalog of Bright Galaxies (de Vaucouleurs et al. 1991).

In the NED, 6 493 galaxies having RVs 3 000 km s^{-1} to 5 000 km s^{-1} were listed until the cutoff date. Morphological information was given in the catalogs for 3 276 (50%) galaxies. We visually inspected all these galaxies using ALADIN2.5 software.

The arm patterns (S- or Z-type) of the galaxies were studied visually by the author in order to maintain homogeneity. The contour maps of the galaxies were studied in order to identify their structural modes. For this, we used ALADIN2.5 software. The Z-mode is one whose outer tip points towards the counterclockwise direction (see Fig. 1(a)). Similarly, the outer tip of the S-mode is directed to the clockwise direction. These two patterns are obviously the two dimensional projections

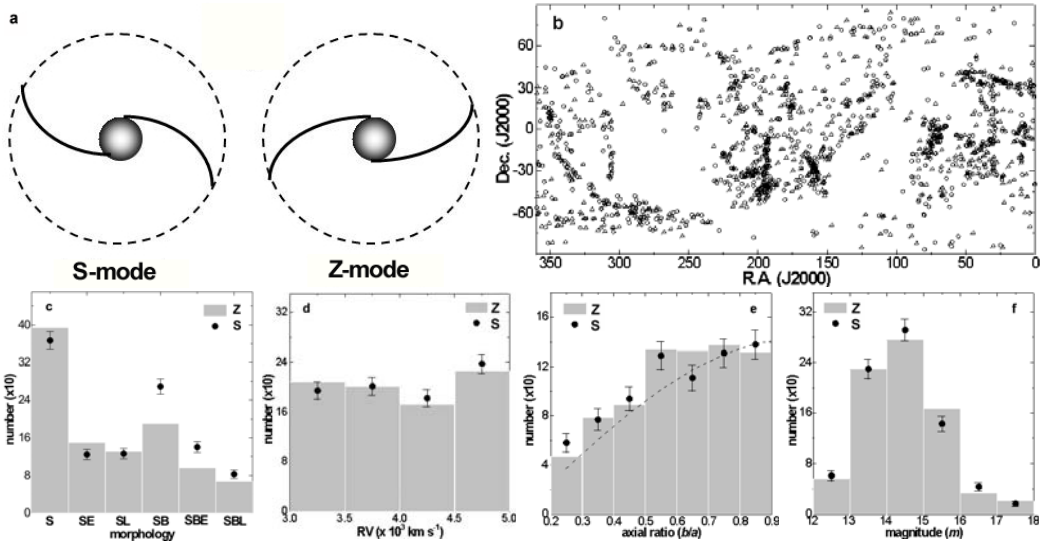

Fig. 1 (a) A sketch representing the winding sense (S or Z) of the galaxy. (b) All-sky distribution of Z-mode (△) and S-mode (○) galaxies that have RVs in the range 3 000 km s^{-1} to 5 000 km s^{-1}. The morphology (c), radial velocity (d), axial ratio (e) and the magnitude (f) distributions of Z- and S-mode galaxies in our database. The statistical $\pm 1\sigma$ error bars are shown for the S-mode (●) subsample. The dashed line (e) represents the expected distribution.

of a three dimensional galaxy. The re-examination of the S- and Z-modes using the MIDAS software resulted in the rejection of more than 17% of the objects. These rejected galaxies were nearly edge-on spiral and barred spiral galaxies. As expected, it was relatively easier to identify the structural modes of nearly face-on galaxies than for nearly edge-on galaxies.

In this way, we compiled a database of 1 621 galaxies showing either S- or Z-structural modes. There were 807 Z-mode and 821 S-mode galaxies in our database. The all sky distribution of Z- and S-mode galaxies is shown in Figure 1(b). The symbols "○" and "△" represent the positions of the S-mode and Z-mode galaxies, respectively. Several groups and aggregations of the galaxies can be seen in the figure.

The morphology, radial velocity, axial ratio and the magnitude distributions of S- and Z-mode galaxies are shown in Figure 1(c)–(f). The spirals (47%) dominate our database (Fig. 1(c)). However, a significant dominance of S-modes is noticed in the barred spirals, whereas a weak dominance of Z-modes is found in the spirals. The population of galaxies in the RV distribution (ΔRV = 500 km s^{-1}) was nearly equal (Fig. 1(d)). The axial ratio distribution shows a good agreement with the expected *cosine* curve in the limit $0.2 < b/a \leq 0.9$ (Fig. 1(e)). The values of absolute magnitude lie between 13.0 and 16.0 for 82% of galaxies in our database (Fig. 1(f)).

We classified the database into 32 subsamples for both the S- and Z-modes on the basis of the morphology, radial velocity, area and the group label of the galaxies. The galaxies with doubtful morphology were omitted from the spiral and barred spiral subsamples. The total number of early- and late-type spirals or barred spirals was much less than that of the total spirals or total barred spirals, which is because of the fact that the galaxy with incomplete morphology, say, simply 'S' or 'SB' cannot be included in the subsamples. In other words, a galaxy with morphology Sa, Sab, Sb, or Sbc is included in the early spirals whereas a galaxy with morphology Sc, Scd, Sd or Sdm is classified as a late type spiral. The galaxies having morphology other than Sa, Sab, Sb, Sbc, Sc, Scd,

Sd and Sm cannot be included in the early or late subsamples. A statistical study of these subsamples is given in Table 1 and is discussed in Section 4.1.

3 METHOD OF ANALYSIS

Basic statistics is used to study the dominance of Z- or S-mode galaxies. At first, morphology and RV dependence are studied. Secondly, the sky is divided into 16 equal parts in order to observe a possible deviation from homogeneity. Several galaxy groups are identified in the all-sky map where the structural dominance is noticed. Finally, we study the dominance of Z- or S-mode galaxies in these groups.

We assume an isotropic distribution as a theoretical reference and study the equatorial PA-distribution in the total sample and subsamples. In order to measure the deviation from the isotropic distribution, we carried out three statistical tests: chi-square, auto-correlation and a Fourier series.

We set the chi-square probability $P(> \chi^2) = 0.050$ as the critical value to discriminate isotropy from anisotropy; this corresponds to a deviation from isotropy at the 2σ level (Godlowski 1993). The auto-correlation test takes into account the correlation between the number of galaxies in adjoining angular bins. We expect the auto-correlation coefficient C$\rightarrow$0 for an isotropic distribution. The critical limit is the standard deviation of the correlation coefficient C.

If the deviation from isotropy is only slowly varying with respect to angle (in our case: PA) the Fourier test can be applied (Godlowski 1993). A method of expanding a function by expressing it as an infinite series of periodic functions (sine and cosine) is called the Fourier series. Let N denote the total number of solutions for galaxies in the sample, N_k the number of solutions in the $k^{\rm th}$ bin, N_0 the mean number of solutions per bin, and N_{0k} the expected number of solutions in the $k^{\rm th}$ bin. Then the Fourier series is given by (taking the first order Fourier mode),

$$N_k = N_k(1 + \Delta_{11}\cos 2\beta_k + \Delta_{21}\sin 2\beta_k + ...), \tag{1}$$

where the angle β_k represents the polar angle in the $k^{\rm th}$ bin. The Fourier coefficients Δ_{11} and Δ_{21} are the parameters of the distributions. We obtain the following expressions for the Fourier coefficients Δ_{11} and Δ_{21},

$$\Delta_{11} = \sum(N_k - N_{0k})\cos 2\beta_k / \sum N_{0k}\cos^2 2\beta_k, \tag{2}$$

$$\Delta_{21} = \sum(N_k - N_{0k})\sin 2\beta_k / \sum N_{0k}\sin^2 2\beta_k. \tag{3}$$

The standard deviations ($\sigma(\Delta_{11})$) and ($\sigma(\Delta_{21})$) can be estimated using the expressions,

$$\sigma(\Delta_{11}) = (\sum N_{0k}\cos^2 2\beta_k)^{-1/2}, \tag{4}$$

$$\sigma(\Delta_{21}) = (\sum N_{0k}\sin^2 2\beta_k)^{-1/2}. \tag{5}$$

The probability that the amplitude

$$\Delta_1 = (\Delta_{11}^2 + \Delta_{21}^2)^{1/2} \tag{6}$$

is greater than a certain chosen value is given by the formula

$$P(> \Delta_1) = \exp(-nN_0\Delta_1^2/4) \tag{7}$$

with standard deviation

$$\sigma(\Delta_1) = (2/nN_0)^{1/2}. \tag{8}$$

The Fourier coefficient Δ_{11} gives the direction of departure from isotropy. The first order Fourier probability function $P(> \Delta_1)$ estimates whether (shown by a smaller value of $P(> \Delta_1)$) or not (shown by a higher value of $P(> \Delta_1)$) a pronounced preferred orientation occurs in the sample.

4 RESULTS

First we present the statistical result concerning the distribution of Z- and S-mode galaxies in the total sample and subsamples. Second, we study the distribution of Z- and S-mode galaxies in the unit area of the sky and in the groups. Then, the equatorial PA-distribution of galaxies in the total sample and subsamples are discussed. At the end, a general discussion and a comparison with the previous results will be presented.

4.1 Distribution of Z and S Mode Galaxies

A statistical comparison between the total sample and subsamples of the Z- and S-modes of galaxies is given in Table 2. Figure 2 shows this comparison in the histogram. The $\Delta(\%)$ in Table 2 and Figure 2 represents the percentage difference between the number of Z- and S-mode galaxies. We studied the standard deviation of the major diameters (a) of galaxies in the total sample and subsamples for both the Z- and S-modes. In Table 2, $\Delta(a\,\mathrm{sde})$ represents the difference between the standard deviations of the major diameters of Z- and S-mode galaxies.

An insignificant difference ($0.4\% \pm 0.2\%$) between the total number of Z- and S-mode galaxies is found (Table 2). The difference between the standard deviation of the major diameters ($\Delta(a\,\mathrm{sde})$) of the Z- and S-mode galaxies is found to be less than 0.019 (eighth column, Table 2). Interestingly, the sum of the major diameters of total Z- and S-mode galaxies coincide. This result suggests there is a homogeneous distribution of Z- and S-mode field galaxies that have RV values in the range $3\,000\,\mathrm{km\ s^{-1}}$ to $4\,000\,\mathrm{km\ s^{-1}}$.

In Figure 2, the slanted-line (grey-shaded) region corresponds to the region showing a $\leq 10\%$ (5%) Δ value. Almost all subsamples lie in this region, suggesting the homogeneous distribution of Z- and S-mode galaxies are within the 10% error limit. Now, we present the distribution of Z- and S-mode galaxies in the subsamples classified according to their morphology, RV, area and associated groups below.

4.1.1 Morphology

In the spirals, Z-mode galaxies are found 3.7% ($\pm 1.8\%$) more than S-mode ones. A homogeneous distribution of Z- and S-modes is found more for the late-type spirals (Sc, Scd, Sd and Sm) than for early-type ones (Sa, Sab, Sb and Sbc): The Δ value turned out to be 9.5% ($\pm 4.8\%$) and 1.8% ($\pm 1.0\%$) for early- and late-types (Table 2), respectively. Thus, no preferred winding pattern is apparent in the late-type spirals compared to the early-type ones.

A significant dominance of S-mode galaxies is noticed ($17\% \pm 8.5\%$) in spiral barred galaxies. The Δ value is found to be $> 9\%$ for both early- (SBa, SBab, SBb and SBbc) and late-type (SBc, SBcd, SBd and SBm) barred spirals. A similar result (i.e., $\Delta > 8\%$) is found for the irregulars and the morphologically unidentified galaxies.

A similarity is noticed between the late-type spirals and barred spirals: the Δ value for both of the late-types is found to be less than that of the early-types (see Table 2).

The difference between the standard deviation of the major diameters ($\Delta(a\,\mathrm{sde})$) for S- and Z-mode galaxies is found to be less than 0.050 arcmin for the whole sample, spirals and late-type spirals (eighth column, Table 2). These samples showed Δ values $<5\%$ (grey-shaded region, Fig. 2(a)). Thus, we noticed a good correlation between the $\Delta(\%)$ and $\Delta(a\,\mathrm{sde})$ value.

The difference between the sum of the major diameters (in percentage) is found to be greater than 10% for the barred spirals and the early-type barred spirals. Interestingly, these two subsamples showed Δ values greater than 15% (Fig. 2(a)). Thus, inhomogeneity in the distribution of S- and Z-mode galaxies is noticed for barred spirals.

Table 2 Statistics of the Total Sample and Subsamples

Sample / Subsample (1)	Symbol (2)	Z (3)	S (4)	Δ (5)	Δ(%) (6)	σ(%) (7)	$\Delta(a$ sde) (8)	$\Delta(a)$(%) (9)
Total	T	814	807	–7	–0.4	–0.2	0.019	0.0
Spiral	S	395	367	–28	–3.7	–1.8	0.031	3.0
Spiral (early-type)	SE	150	124	–26	–9.5	–4.8	0.058	8.1
Spiral (late-type)	SL	131	126	–5	–1.9	–1.0	0.031	0.3
Barred Spiral	SB	191	269	78	17.0	8.5	0.062	15.2
Barred Spiral (early-type)	SBE	97	140	43	18.1	9.1	0.091	14.6
Barred Spiral (late-type)	SBL	68	83	15	9.9	5.0	0.066	9.2
3 000<RV (km s^{-1})≤3 500	RV1	208	194	–14	–3.5	–1.7	0.046	2.6
3 500<RV (km s^{-1})≤4 000	RV2	201	201	0	0.0	0.0	0.031	3.1
4 000<RV (km s^{-1})≤4 500	RV3	172	182	10	2.8	1.4	0.034	0.6
4 500<RV (km s^{-1})≤5 000	RV4	226	237	11	2.4	1.2	0.041	1.0
Grid 1	G1	20	21	1	2.4	1.2	0.068	6.8
Grid 2	G2	121	116	–5	–2.1	–1.1	0.014	1.6
Grid 3	G3	88	112	24	12.0	6.0	0.076	9.3
Grid 4	G4	12	14	2	7.7	3.9	0.647	9.7
Grid 5	G5	11	8	–3	–15.8	–7.9	0.042	22.3
Grid 6	G6	75	80	5	3.2	1.6	0.081	4.5
Grid 7	G7	62	56	–6	–5.1	–2.5	0.095	8.9
Grid 8	G8	22	33	11	20.0	10.1	0.073	12.9
Grid 9	G9	20	31	11	21.6	10.9	0.028	18.1
Grid 10	G10	124	108	–16	–6.9	–3.5	0.004	5.4
Grid 11	G11	61	52	–9	–8.0	–4.0	0.025	6.2
Grid 12	G12	20	20	0	0.0	0.0	0.409	7.4
Grid 13	G13	78	66	–12	–8.3	–4.2	0.039	2.9
Grid 14	G14	37	44	7	8.6	4.3	0.356	10.3
Grid 15	G15	47	44	–3	–3.3	–1.6	0.050	5.2
Grid 16	G16	9	9	0	0.0	0.0	0.191	8.6
Group 1	Gr1	37	30	–7	–10.4	–5.2	0.032	7.1
Group 2	Gr2	48	70	22	18.6	9.4	0.097	12.6
Group 3	Gr3	31	37	6	8.8	4.4	0.027	4.3
Group 4	Gr4	34	40	6	8.1	4.1	0.031	3.9
Group 5	Gr5	107	85	–22	–11.5	–5.7	0.089	11.2
Group 6	Gr6	42	45	3	3.4	1.7	0.024	1.6

The sample/subsample and their abbreviations are given in the first two columns. Statistics of leading (Col. (3)) and trailing arm (Col. (4)) galaxies in the total sample and subsamples are listed, respectively. The fifth and sixth columns give the numeral and percentage difference ($\Delta = S–Z$) between the S- (S) and the Z- (Z) modes. The next two columns give the errors: $\sigma = (\sqrt{S}–\sqrt{Z})$ and $\sigma(\%) = \sigma/(\sqrt{S}+\sqrt{Z})\times 100$. The eighth column gives the difference between the standard deviation (in arcmin) of the major diameters (a) of the S- and Z-mode galaxies ($\Delta(a$ sde)). The difference between the sum of the major diameters ($\Delta(a)\%$) is listed in the last column.

4.1.2 Radial velocity

A very good correlation between the number of S- and Z-modes can be seen in the RV classifications (Fig. 1(d)). All four subsamples show Δ and $\Delta(a$ sde) values less than 5% and 0.050, respectively (Table 2). In addition, $\Delta(a)$ is found to be <5%. This result is important in the sense that the statistics in these subsamples is rich enough (number of galaxies >170). Thus, we could not observe preferred structural modes (S or Z) in the low or high RV galaxies in our database.

A difference is noticed: the dominance of Z- and S- modes, respectively, in low (RV1) and high (RV3, RV4) RV subsamples. However, this dominance is not significant (i.e., Δ <5%). An equal number of S- and Z-mode galaxies is found in the subsample RV2 (3 500 <RV (km s^{-1}) ≤ 4 000) (Table 1). In order to check the binning effect, we further classify the total galaxies into six (ΔRV = 333 km s^{-1}) and eight bins (ΔRV = 250 km s^{-1}) and study the statistics. No significant dominance of either S- or Z-modes is noticed.

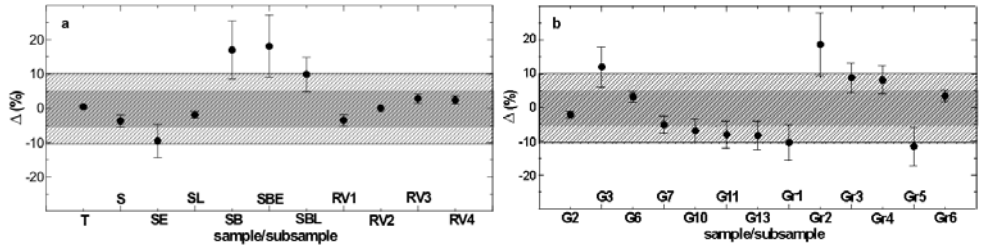

Fig. 2 Basic statistics of the Z- and S-mode of galaxies in the total sample and subsamples. The full form of the abbreviations (X-axis) are given in Table 2 (first column). $\Delta(\%)=S-Z$, where S and Z represent the number of S- and Z-mode galaxies, respectively. The statistical error bars $\sigma(\%)$ shown in the figure are calculated as: $\sigma(\%) = \sigma/(\sqrt{S}+\sqrt{Z})\times 100$, where $\sigma = (\sqrt{S}-\sqrt{Z})$. The grey-shaded and the slanted-line regions represent the $\leq\pm 5\%$ and $\leq\pm 10\%$ Δ values, respectively.

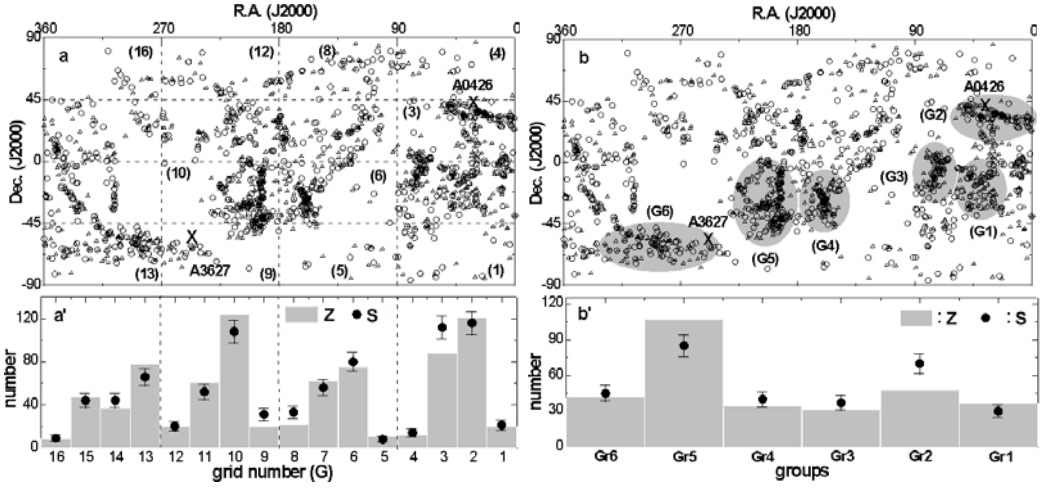

Fig. 3 (a) All sky distribution of Z-mode (*hollow circle*) and S-mode (*hollow triangle*) galaxies in 16 area grids. (a′) The histogram showing the distribution of the Z- and S-mode galaxies in the grids G1 to G16. (b) Six groups of these galaxies, represented by the grey-shaded region. (b′) The distribution of Z- and S-modes in six groups. The statistical error bar $\pm 1\sigma$ is shown. The positions of the clusters Abell 0426 and Abell 3627 are shown by the symbol "×" (a, b).

Thus, it is found that the homogeneous distribution of S- and Z-mode galaxies remains invariant with the global expansion (i.e, expansion of the Universe). We further discuss this result below.

4.1.3 Area

We study the distribution of S- and Z-mode galaxies by dividing the sky into 16 equal parts (Fig. 3(a)). The area of the grid (G) is 90° × 45° (RA × Dec). The area distribution of S- and Z-mode galaxies is plotted, which can be seen in Figure 3(a′). The statistical parameters are given in Table 2.

A significant dominance ($>2\sigma$) of S-mode is noticed in grid 3 (RA: 0° to 90°, Dec: 0° to 45° (J2000)) (Fig. 3(a) and (a′)). An elongated group of galaxies can be seen. In this grid, Δ, $\Delta(a\,\mathrm{sde})$ and $\Delta(a)\%$ are found to be $12\% \pm 6\%$, 0.076 and 9.3%, respectively. These figures suggest that the distribution of S- and Z-mode galaxies in G3 is not homogeneous. Probably, this is due to the apparent subgroupings or subclusterings of the galaxies.

The S-mode galaxies dominate in the grids G8 and G9 (Fig. 3(a′)). However, the statistics is poor (<40) in these grids (Table 2). In addition, no groupings or subclusterings are noticed.

A dominance ($\sim 1.5\sigma$) of Z-mode is noticed in G10 (RA: 180° to 270°, Dec: –45° to 0° (J2000)) and G13 (RA: 270° to 360°, Dec: –90° to –45° (J2000)) (Fig. 3(a) and (a′)). In both the grids, a large aggregation of the galaxies can be seen. A subcluster-like aggregation can be seen in G10. An elongated structure can be seen in G13. In both the grids, the Δ value is found to be greater than 5% (Table 2).

No dominance of either S- or Z-mode galaxies is noticed in the groups G1, G2, G4, G5, G6, G7, G11, G12, G14, G15 or G16. Thus, a homogeneous distribution of S- and Z-mode galaxies is found to be intact in $\sim 80\%$ of the area in the sky that was surveyed. We suspect that the groupings or subclusterings of the galaxies lead to preferred structural modes (S or Z) in G3, G10 and G13.

4.1.4 Galaxy groups

In the all-sky map, several groups of galaxies can be seen (Fig. 3(a)). It is interesting to study the distribution of structural modes (S or Z) of galaxies in these groups. For this, we systematically searched for the groups fulfilling the following selection criteria: (a) major diameter $>30°$, (b) cutoff diameter <2 times the background galaxies, (c) number of galaxies >50. We found six groups fulfilling these criteria (Fig. 3(b)). All six groups (Gr) were inspected carefully. In three groups (Gr2, Gr5 and Gr6), subgroups can be seen. The number of galaxies in groups Gr2 and Gr5 were found to be more than 100.

The clusters Abell 0426 and Abell 3627 are located close to the groups Gr2 and Gr6. The symbol "$\times$" represents the position of the cluster center in Figure 3(b). The mean radial velocities of these clusters are 5 366 km s^{-1} and 4 881 km s^{-1}, respectively. However, we have removed the member galaxies of these clusters from our database.

A significant dominance ($>2\sigma$) of S-mode galaxies is noticed in group Gr2 (Fig. 3(b) and (b′)). The Δ, $\Delta(a\,\mathrm{sde})$ and $\Delta(a)\%$ values are found to be 18.6% ($\pm$9.4%), 0.097 and 12.6%, respectively (Table 2). We suspect that the galaxies in this group are under the influence of the cluster Abell 0426, due to which, the apparent subclustering of the galaxies can be seen.

The galaxies in Gr5 show an opposite preference: a significant dominance of the Z-mode galaxies ($>2\sigma$) (Fig. 3(b) and (b′)). In this group, Δ, $\Delta(a\,\mathrm{sde})$ and $\Delta(a)\%$ are found to be $11.5\% \pm 5.7\%$, 0.089 and 11.2%, respectively, suggesting an inhomogeneous distribution of structural modes (Table 2).

No humps or dips can be seen in the groups Gr1, Gr3, Gr4 or Gr6 (Fig. 3(b) and (b′)). Thus, the distribution of S- and Z-mode galaxies in these groups is found to be homogeneous. The number of galaxies in these groups is less than 100.

In the group Gr6, we did not notice any influence from the cluster Abell 3627. This might be due to the offset location of the cluster center from the group center.

4.2 Anisotropy in the Position Angle Distribution

We study the equatorial PA distribution of S- and Z-mode galaxies in the total sample and respective subsamples. A spatially isotropic distribution is assumed in order to examine non-random effects in the PA-distribution. In order to discriminate the deviation from randomness, we use three statistical tests: chi-square, auto-correlation and Fourier series. The bin size was chosen to be 20° (nine bins) in

all of these tests. The statistically poor bins (number of solutions <5) are omitted in the analysis. The conditions for anisotropy are the following: the chi-square probability $P(>\chi^2) < 0.050$, correlation coefficient $C/\sigma(C)$ >1, first order Fourier coefficient $\Delta_{11}/\sigma(\Delta_{11})$ >1 and the first order Fourier probability $P(>\Delta_1)$ <0.150, as used by Godlowski (1993). Table 3 lists the statistical parameters for the total samples and subsamples.

Table 3 Statistics of the PA-distribution of Galaxies in the Total Sample and Subsamples

Sample	S-mode				Z-mode			
(1)	$P(>\chi^2)$ (2)	C/C(σ) (3)	$\Delta_{11}/\sigma(\Delta_{11})$ (4)	$P(>\Delta_1)$ (5)	$P(>\chi^2)$ (6)	C/C(σ) (7)	$\Delta_{11}/\sigma(\Delta_{11})$ (8)	$P(>\Delta_1)$ (9)
total	0.666	+0.0	–0.9	0.381	0.015	–3.2	–1.9	0.085
S	0.511	–0.7	–1.2	0.434	0.225	+0.4	+0.8	0.383
SE	0.973	+0.1	–0.9	0.569	0.031	+2.0	+2.8	0.015
SL	0.234	+0.5	+0.8	0.209	0.460	–0.1	–0.5	0.345
SB	0.729	+0.3	+1.0	0.454	0.285	–1.0	–0.2	0.497
SBE	0.739	+0.1	–0.5	0.566	0.230	–0.7	+0.1	0.521
SBL	0.043	+1.8	+1.7	0.046	0.620	–0.9	–0.2	0.872
RV1	0.910	+0.3	+0.8	0.362	0.369	–0.9	–0.6	0.285
RV2	0.790	+0.3	–1.0	0.496	0.925	–0.4	–0.2	0.887
RV3	0.050	+1.6	–1.5	0.083	0.033	–1.8	–2.3	0.046
RV4	0.043	–2.3	–1.5	0.116	0.636	+0.2	–0.7	0.692
Gr2	0.455	+0.6	+0.8	0.861	0.033	–1.8	+1.7	0.116
Gr5	0.033	–1.4	–2.0	0.085	0.516	+0.4	–0.4	0.548

The second, third, fourth and fifth columns give the chi-square probability ($P(>\chi^2)$), correlation coefficient (C/C(σ)), first order Fourier coefficient ($\Delta_{11}/\sigma(\Delta_{11})$), and first order Fourier probability $P(>\Delta_1)$, respectively. The last four columns use the same labels as the previous columns.

In the Fourier test, Δ_{11} <0 (i.e., negative) indicates an excess of galaxies with the galactic planes parallel to the equatorial plane. In other words, a negative Δ_{11} suggests that the rotation axis of galaxies tends to be oriented perpendicular with respect to the equatorial plane. Similarly, Δ_{11} >0 (i.e., positive) indicates that the rotation axis of the galaxies tends to lie in the equatorial plane.

In the histograms (see Figs. 4–7), a hump at $90^\circ \pm 45^\circ$ (grey-shaded region) suggests that the galactic planes of galaxies tend to lie in the equatorial plane. In other words, the rotation axis of galaxies tends to be oriented perpendicular with respect to the equatorial plane when there is an excess number of solutions in the grey-shaded region in the histogram.

All three statistical tests show isotropy in the total S-mode galaxies. Thus, no preferred alignment is observed for the set of S-mode galaxies (solid circles in Fig. 4(a)). Interestingly, all three statistical tests show anisotropy in the set of Z-mode galaxies. The chi-square and Fourier probabilities ($P(>\chi^2)$, $P(>\Delta_1)$) are found to be 1.5% (<5% limit) and 8.5% (< 15% limit), respectively (Table 2). The auto-correlation coefficient (C/C(σ)) turned out to be –3.2 ($\gg$1). The $\Delta_{11}/\sigma(\Delta_{11})$ value is found to be negative at the $\sim 2\sigma$ level, suggesting that the rotation axes of Z-mode galaxies tend to be oriented perpendicular with respect to the equatorial plane. Three humps at 50° (>1.5σ), 90° (>2σ) and 130° (1.5σ) support this result (Fig. 4(a)). We checked the bias in the results due to bin size by increasing and decreasing the number of bins. A similar statistical result is found for both structural modes. Figure 4(b) shows the PA-distribution histogram for the total sample in 18 bins. The Z-mode galaxies show three significant humps in the grey-shaded region, supporting the results mentioned above.

Thus, we find isotropy for the S-mode galaxies but anisotropy for the Z-mode ones in the total sample.

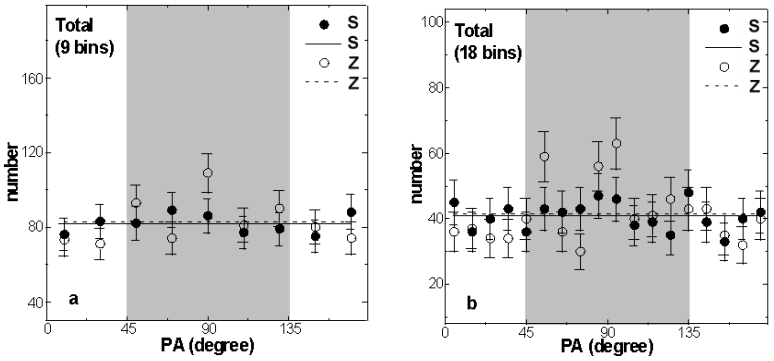

Fig. 4 Equatorial position angle (PA) distribution of all the Z- and S-mode galaxies plotted in 9 (a) and 18 (b) bins. The solid and the dashed lines represent the expected isotropic distribution for S- and Z-mode galaxies, respectively. The observed counts with statistical $\pm 1\sigma$ error bars are shown. PA = $90^\circ \pm 45^\circ$ (*grey-shaded region*) corresponds to the galactic rotation axes tending to be oriented perpendicular with respect to the equatorial plane.

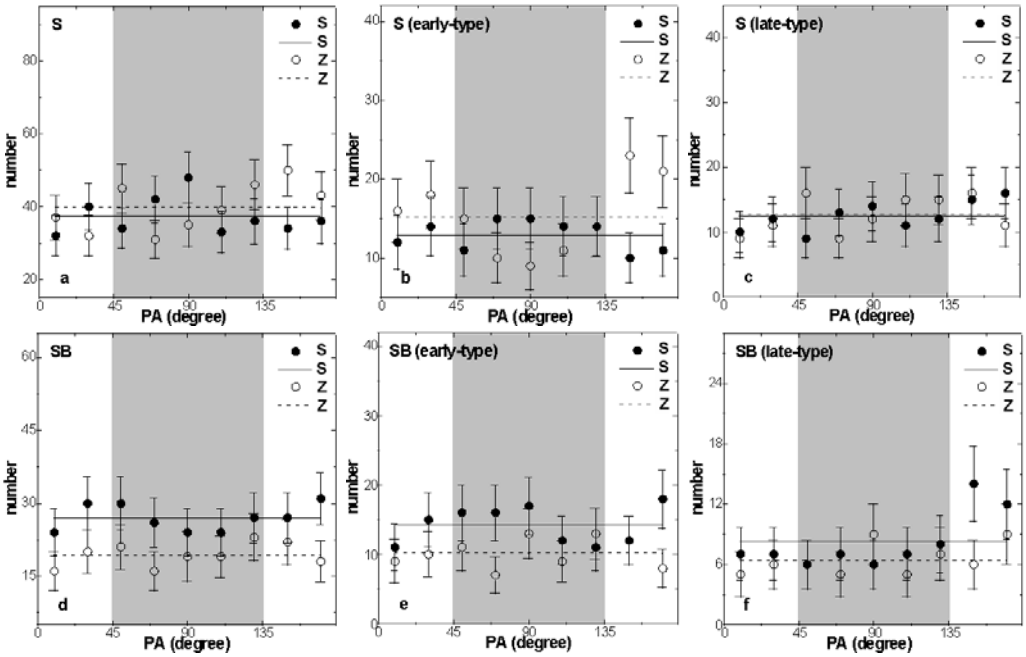

Fig. 5 Equatorial PA-distribution of Z- and S-mode galaxies in the spirals (a), early-type spirals (b), late-type spirals (c), barred spirals (d), early-type barred spirals (e) and late-type barred spirals (f). The symbols, error bars, dashed lines and explanations are analogous to Fig. 4.

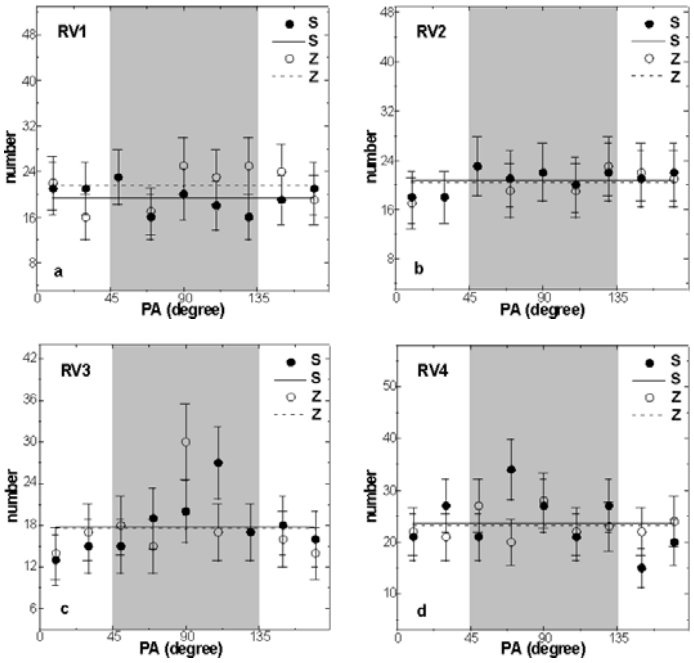

Fig. 6 Equatorial PA-distribution of Z- and S-mode galaxies in RV1 (a), RV2 (b), RV3 (c) and RV4 (d). The abbreviations are listed in Table 1. The symbols, error bars, dashed lines and explanations are analogous to Fig. 4.

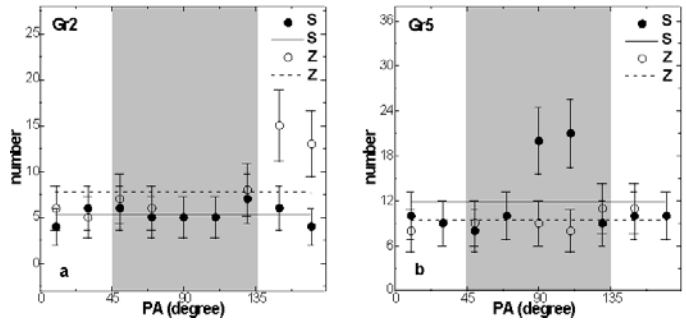

Fig. 7 Equatorial PA-distribution of Z- and S-mode galaxies in groups Gr2 and Gr5. The abbreviations are listed in Table 1. The symbols, error bars, dashed lines and the associated explanations are analogous to Fig. 4.

4.2.1 Morphology

In the spirals, the chi-square and auto-correlation tests show isotropy for both the S- and Z-modes. The first order Fourier probability is found to be greater than 35%, suggesting there is no preferred alignment. However, the Δ_{11} value exceeds the 1σ limit (-1.2σ) in the S-mode spirals. A hump at 90° is not enough to make the value $\Delta_{11}/\sigma(\Delta_{11}) > 1.5$ (Fig. 5(a)). Similarly, a hump at 150° is not enough to make the $\Delta_{11}/\sigma(\Delta_{11}) > 1.5$ in the Z-mode spirals. Hence, the preferred alignment is not

pronounced in both the S- and Z-mode spirals. Thus, we conclude there is a random orientation of S- and Z-mode spirals.

Early- and late-type S-mode spirals show isotropy in all three statistical tests (Table 3). No humps or dips are seen in the figure (solid circles in Fig. 5(b) and (c)). Thus, the S-mode spirals show a random alignment in the PA-distribution. In the subsample SE, all three statistical tests show anisotropy (Table 2). Two significant humps at $>150^\circ$ cause the first order Fourier coefficient (Δ_{11}) $>+2.5\sigma$ (hollow circle in Fig. 5(b)). Thus, a preferred alignment is noticed in the early-type Z-mode spirals: the galactic rotation axes tend to lie in the equatorial plane. The late-type Z-mode spirals show a random alignment.

The barred spiral galaxies show a random alignment in both the S- and Z-modes. In Figure 5(d), no deviation from the expected distribution can be seen. All the three statistical tests support this result (Table 2). A similar result is found for the early-type SB galaxies in both structural modes (Table 3, Fig. 5(e)).

The $P(>\chi^2)$ and $P(>\Delta_1)$ are found to be less than 5%, suggesting a preferred alignment for the late-type S-mode SB galaxies (Table 3). The auto-correlation coefficient (C/C(σ)) and the hump at $>150^\circ$ support this result (Fig. 5(f)). The $\Delta_{11}/\sigma(\Delta_{11})$ is found to be positive at the 1.7σ level, suggesting that the S-mode late barred spiral galaxies tend to lie in the equatorial plane. Thus, the late-type S- and Z-mode SB galaxies show preferred and random alignments, respectively.

4.2.2 Radial velocity

The subsamples RV1 and RV2 show isotropy in all three statistical tests (Table 2). No humps or dips can be seen in Figure 6(a) and (b). Thus, the galaxies having radial velocity in the range 3 000 km s^{-1} to 4 000 km s^{-1} show a random alignment for both the S- and Z-mode galaxies.

The humps at 90° ($>2\sigma$) and 110° ($>2\sigma$) are found in the Z- and S-mode RV3 galaxies, respectively (Fig. 6(c)). These two significant humps cause the subsample to show anisotropy in the statistical tests (Table 2). The Δ_{11} values are found to be negative at the $\geq$1.5 level, suggesting a similar preferred alignment for both modes: the galaxy rotation axes tend to be directed perpendicular with respect to the equatorial plane.

A hump at 70° ($>1.5\sigma$) and a dip at 150° ($\sim 2\sigma$) cause the S-mode RV4 galaxies to show anisotropy in all three statistical tests (Fig. 6(d)). Thus, the S-mode galaxies having radial velocity in the range 4 500 km s^{-1} to 5 000 km s^{-1} show a similar preferred alignment as shown by the subsample RV3: galactic planes of galaxies tend to lie in the equatorial plane. The leading arm galaxies in the subsample RV4 show a random alignment (Table 3, Fig. 6(d)).

4.2.3 Groups

We do not study PA-distribution of S- and Z-mode galaxies in the groups Gr1, Gr3, Gr4 and Gr6 because of poor statistics (number $<$50).

We study the PA-distribution of S- and Z-mode galaxies in the groups Gr2 and Gr5, where the dominance of either Z- or S-mode is apparent. In addition, the statistics is relatively better in these groups.

In the group Gr2, Z-mode galaxies dominate the S-mode galaxies. In this group, the Z-mode galaxies show a preferred alignment whereas S-mode galaxies show a random alignment in the PA-distribution. All three statistical tests suggest anisotropy in the Z-mode galaxies (Table 3). The humps at $>150^\circ$ cause the Δ_{11} value to be positive at the $>1.5\sigma$ level (Fig. 7(a)), suggesting that the rotation axes of Z-mode galaxies in Gr2 tend to be oriented parallel to the equatorial plane.

The S-mode galaxies dominate in the group Gr5. Interestingly, a preferred alignment of S-mode galaxies is noticed in the PA-distribution. In Figure 7(b), two significant humps at 90° ($\sim 2\sigma$) and

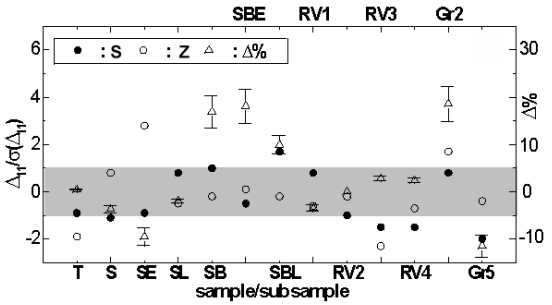

Fig. 8 A comparison between the number ($\Delta\%$) and the position angle ($\Delta_{11}/\sigma(\Delta_{11})$) distribution of Z- and S-mode galaxies in the total sample and the respective subsamples.

110° ($>2\sigma$) can be seen. These humps lead the subsample (S-mode Gr5) to show anisotropy in the statistical tests (Table 3). No preferred alignment is noticed in the Z-mode galaxies of this group.

Thus, the dominant structural modes (Z or S) show a preferred alignment in the PA-distribution. This is a significant result.

4.3 Discussion

Figure 8 shows a comparison between the number (Δ) and position angle ($\Delta_{11}/\sigma(\Delta_{11})$) distribution of S- and Z-mode galaxies in the total sample and the respective subsamples. This plot displays the correlation between the homogeneity in the structural modes and the random alignment in the subsamples. The grey-shaded region represents the region of isotropy and homogeneity for the $\Delta_{11}/\sigma(\Delta_{11})$ and $\Delta(\%)$, respectively. Twenty-five (out of 39, 64%) of the subsamples lie in the grey-shaded region (Fig. 8(a)), suggesting there is a good agreement between the homogeneous distribution of S- and Z-mode galaxies and the random alignment of the rotation axes of galaxies. In four subsamples (SE, SBL, Gr2 and Gr5), a good correlation between the preferred alignment and the dominance of either S- or Z-mode galaxies is apparent (Fig. 8). Thus, it is noticed that the random alignment of the PAs of galaxies hints at the existence of inhomogeneity in the structural modes.

Aryal & Saurer (2006) and Aryal et al. (2007) studied the spatial orientation of galaxies in 32 Abell clusters of BM type I, II, II-III and III and found a significant preferred alignment in the late-type cluster (BM type II-III, III). They concluded that the randomness decreases systematically in galaxy alignments from early-type (BM type I, II) to late-type (BM type II-III, III) clusters.

We observed a very good correlation between the random alignments and the homogeneity in the structural modes. Probably, this result reveals the fact that the progressive loss of homogeneity in the structural modes might have some connection with progression from the rotationally supported cases (spirals, barred spirals) to the randomized (lenticulars, ellipticals) systems. Thus, we suspect that the dynamical processes in the cluster evolution (such as late-type clusters) give rise to a dynamical loss of homogeneity in the structural modes. It would be interesting to test this prediction by studying the S- and Z-type spirals in the late-type clusters in the future.

Since 60% of galaxies in the nearby universe are rotationally supported disks, understanding their angular-momentum acquisition is obviously a crucial part of understanding the galaxys' evolution. The winding sense of spiral arm patterns (morphological feature) allows us to infer the orientation of the angular-momentum vector of the disk galaxy. The expected distribution of spin vectors of galaxies shows markedly different trends according to the galaxy formation scenarios. One can suspect the possibility that the actual distribution of galaxy spin shows a dipole or a quadrupole component depending on the scenarios of galaxy formation. If galaxy spins were generated according to

the primordial whirl scenario, a strong bias in either the S or Z patterns would be seen in a face-on sample of galaxies. We did not find this trend in our sample. A quadrupole distribution of S/Z might be observed if the primary process was the generation of spins due to the pancake shock scenario or the explosion scenario. On the other hand, if the galaxy spins were produced by the tidal spin-up process, there would be no global anisotropy as we noticed in many cases, unless galaxy-cluster tidal interaction rather than galaxy-galaxy tidal interaction were the primary process. No significant correlation, however, was identified in any ensemble.

5 CONCLUSIONS

We studied the winding sense of 1 621 field galaxies around the Local Supercluster. These galaxies have radial velocities (RVs) in the range 3 000 km s^{-1} to 5 000 km s^{-1}. The distribution of Z- and S-mode galaxies is studied in the total sample and in 32 subsamples. To examine non-random effects, the equatorial PA distribution of galaxies in the total sample and subsamples is studied. In order to discriminate anisotropy from possible isotropy, we have performed three statistical tests: chi-square, auto-correlation and Fourier series. Our results are as follows:

1. The homogeneous distribution of the total Z- and S-mode galaxies is found, suggesting there exists a homogeneous distribution of the winding sense (S or Z) of galaxies having RVs 3 000 km s^{-1} to 5 000 km s^{-1}. The PA-distribution of S-mode galaxies is found to be random, whereas a preferred alignment is noticed for Z-mode galaxies. It is found that the galactic rotation axes of Z-mode galaxies tend to be oriented perpendicular to the equatorial plane.
2. Z-mode cases are found 3.7% ($\pm$1.8%) more than S-mode ones in spirals, whereas a significant dominance (17% $\pm$ 8.5%) of S-mode cases is noticed in barred spirals. This difference is found to be $>$8% for irregulars and morphologically unidentified galaxies. A random alignment is noticed in the PA-distribution of Z- and S-mode spirals. Thus, it is noticed that the random alignment of the PAs of galaxies leads to the existence of inhomogeneity in the structural modes of galaxies.
3. The inhomogeneity in the structural modes is found to be stronger for late-type spirals (Sc, Scd, Sd and Sm) than for early-type ones (Sa, Sab, Sb and Sbc). A similar result is found for late-type barred spirals.
4. A very good correlation between the number of Z- and S-mode galaxies is found in the RV subsamples. All four subsamples show the Δ value to be less than 5%. Thus, we conclude that the homogeneous distribution of structural modes of field galaxies remains invariant with the global expansion.
5. The galaxies having RVs 3 000 km s^{-1} to 4 000 km s^{-1} show a random alignment for both the Z- and S-modes. The rotation axes of Z- and S-mode galaxies having 4 000 $<$ RV (km s^{-1}) $\leq$ 4 500 tend to be oriented perpendicular to the equatorial plane.
6. The distribution of the winding sense of galaxies is found to be homogeneous in $\sim$ 80% of the area in the sky. However, this property is found to be violated in a few groups of galaxies. Two such groups (Gr2 and Gr8) are identified. In these groups, the structural dominance and the preferred alignments of galaxies are found to oppose each other.

The true structural mode of a galaxy must involve a determination of which side of the galaxy is closer to the observer (Binney & Tremaine 1987). Three-dimensional determination of the leading and the trailing arm patterns in the galaxies is a very important problem. We intend to address this problem in the future.

Acknowledgements We are indebted to the referee for his/her constructive criticism and useful comments. I acknowledge Profs. R. Weinberger and W. Saurer of Innsbruck University, Austria for their insightful discussions. I am thankful to Tribhuvan University, Nepal and Innsbruck University, Austria for providing financial assistance to visit Innsbruck University during January-March 2009.

References

Abell, G. O., Corwin, H. G., Jr., & Olowin, R. P. 1989, ApJS, 70, 1
Aryal, B., Paudel, S., & Saurer, W. 2007, MNRAS, 379, 1011
Aryal, B., & Saurer, W. 2006, MNRAS, 366, 438
Aryal, B., & Saurer, W. 2005, A&A, 432, 841
van den Bergh, S. 1959, Publ. David Dunlop Obs. 2, 145
van den Bergh, S. 1966, AJ, 71, 922
Binney, J., & Tremaine, S. 1987, Galactic Dynamics (Princeton, NJ: Princeton Univ. Press),747
Brandner, W., Grebel, E. K., Chu, Y.-H., et al. 2000, AJ, 119, 292
Brunzendorf, J., & Meusinger, H. 1999, A&AS, 139, 141
Capozziello, S., & Lattanzi, A. 2006, Ap&SS, 301, 189
Corwin, H. G., de Vaucouleurs, A., & de Vaucouleurs, G. 1985, Univ. Texas Monogr. Astron., 4, 1
Dreyer, J. L. E. 1895, MmRAS, 51, 185
Dreyer, J. L. E. 1908, MmRAS, 59, 105
Doroshkevich, A. G. 1973, Astrophys. Lett., 14, 11
de Vaucouleurs, G., de Vaucouleurs, A., Corwin, H. G., Jr., et al. 1991, Third Reference Catalogue of Bright Galaxies (New York: Springer-Verlag)
Godlowski, W. 1993, MNRAS, 265, 874
Impey, C. D., Sprayberry, D., Irwin, M. J., & Bothun, G. D. 1996, ApJS, 105, 209
Kodaira, K., Okamura, S., & Ichikawa, S. 1990, Photometric Atlas of Northern Bright Galaxies, eds. K. Kodaira, S. Okamura, & S. Ichikawa (Tokyo: Univ. of Tokyo Press)
Land, K., Slosar, A., Lintott, C., et al. 2008, MNRAS, 388, 1686
Lauberts, A. 1982, ESO/Uppsala Survey of the ESO B Atlas, Garching bei Muenchen
Longo, M. J. 2007, arXiv:astro-ph/0703325
MacAlpine, G. M., Smith, S. B., & Lewis, D. W. 1977a, ApJS, 34, 95
MacAlpine, G. M., Smith, S. B., & Lewis, D. W. 1977b, ApJS, 35, 197
MacAlpine, G. M., Lewis, D. W., & Smith, S. B. 1977c, ApJS, 35, 203
MacAlpine, G. M., & Lewis, D. W. 1978, ApJS, 36, 587
MacAlpine, G. M., & Williams, G. A. 1981, ApJS, 45, 113
Markarian, B. E. 1967, Astrofizika, 3, 24
Markarian, B. E., Lipovetskii, V. A., & Stepanian, D. A. 1983, Astrofizika, 19, 29
Messier, C. 1784, Catalogue des nebuleuses et des amas d'etoiles, Connaissance des Temps
Nilson, P. 1973, Uppsala General Catalogue of Galaxies, Nova Acta Uppsala University, Ser. V:A, Vol.1
Nilson, P. 1974, Upps. Astron. Obs. Rep., 5
Oort, J. H. 1970a, Science, 170, 1363
Oort, J. H. 1970b, A&A, 7, 405
Ozernoy, L. M. 1978, in Proc. IAU Symp. 79, The Large Scale Structure of the Universe, eds. M. S. Longair, & J. Einasto (Dordrecht: D. Reidel Publishing Co.), 427
Peebles, P. J. E. 1969, ApJ, 155, 393
Pasha, I. I. 1985, Sov. Astron. Lett., 11, 1
Shectman, S. A., Landy, S. D., Oemler, A., et al. 1996, ApJ, 470, 172
Struble, M. F., & Rodd, H. J. 1999, ApJS, 125, 35
Sugai, H., & Iye, M. 1995, MNRAS, 276, 327
Takase, et al. 1980–2000, Kiso Ultraviolet Galaxy Catalog, Publ. Nat. Astron. Obs. Japan
Thomasson, M., Donner, K. J., Sundelius, B., et al. 1989, A&A, 211, 25
Vorontsov-Vel, Y. B. A., Krasnogorskaya, A. A., & Arkhipova, V. P. 1962–1974, Morphological Catalogue of Galaxies (Part I-V), Trudy Gosud. Astron. Inst. Shternberga
Zwicky, F., Wild, P., Karpowicz, M., & Kowal, C. T. 1961–1968, The Catalogue of Galaxies and Clusters of Galaxies, California Inst. of Tech., Pasadena